

Rigid assembly and Monte Carlo models of stable and unstable chromatin structures: the effect of nucleosomal spacing

Frank Aumann · Jürgen Sühnel · Jörg Langowski ·
Stephan Diekmann

Received: 12 January 2009 / Accepted: 14 March 2009 / Published online: 4 April 2009
© Springer-Verlag 2009

Abstract Coarse-grained models are used to assess the packing of the 30-nm chromatin fiber. First, rigid assembly models for nucleosomal repeats from 155 to 211 bp are built using the crystal structure of the mononucleosome and attached straight stretches of B-DNA. The resulting fiber conformations are analyzed for static clashes and classified into stable and unstable structures. The effect of flexibility and thermal fluctuations is then taken into account by conducting Monte Carlo simulations of chromatin fiber models. Here the DNA is approximated by a flexible polymer chain with Debye–Hückel electrostatics, the geometry of the linker DNA connecting the nucleosomes is based on a two-angle zigzag model, and nucleosomes are represented by flat ellipsoids interacting via an attractive Gay–Berne potential. Unstable fibers occur at a particular repeat length period of 10 bp. Also, the regions of densely compacted fibers repeat at intervals

of 10 bp. Besides one- and two-start helical zigzag structures, we show evidence for possible three-start structures, which have not been reported in experiments yet. Finally, we show that a local opening of the linker DNA at the nucleosome core—as probably occurs upon histone acetylation—leads to more open and flexible structures.

Keywords Chromatin fiber · Monte Carlo simulation · Rigid assembly model · Repeat length · Quantization · Elasticity

Abbreviations

NCP Nucleosome core particle
 L_p Persistence length
MC Monte Carlo

1 Introduction

In eukaryotic cells, DNA is packed into chromatin in a hierarchical process. At the lowest level of compaction, histones bind to DNA and form nucleosomes [1, 2]. Slightly less than two turns of DNA are wrapped around the histone octamer core: one histone octamer and 146 bp DNA form a biochemically stable unit (the “core particle”). The spacing between successive nucleosomes is 160–240 bp depending on the cell type and species. The crystal structures of the histone octamer [3] and the full nucleosome core particle [4] have been solved at atomic resolution. The next packaging level is less well understood. Electron microscopy images of chromatin preparations typically present a 10-nm thick ‘bead-chain’ fiber in hypotonic medium and a 30-nm fiber under physiological conditions [5]. Several models have been proposed to explain the folding of the nucleosome chain

Dedicated to Professor Sandor Suhai on the occasion of his 65th birthday and published as part of the Suhai Festschrift Issue.

F. Aumann and J. Sühnel contributed equally.

Electronic supplementary material The online version of this article (doi:10.1007/s00214-009-0561-9) contains supplementary material, which is available to authorized users.

F. Aumann · J. Langowski
Division Biophysics of Macromolecules,
German Cancer Research Center, Im Neuenheimer Feld 580,
69120 Heidelberg, Germany

J. Langowski
e-mail: jl@dkfz.de

J. Sühnel · S. Diekmann (✉)
Leibniz Institute for Age Research, Fritz Lipmann Institute
(FLI), Beutenbergstraße 11, 07708 Jena, Germany
e-mail: diekmann@fli-leibniz.de

into the 30-nm fiber. They can be grouped into two classes: (1) a one-start helix with bent linker DNA connecting each pair of nucleosome cores following each other immediately along the same helical path (for example, the “solenoid” [6–9]) and (2) a two-start helix with straight linker DNA connecting nucleosome cores which are arranged in two independent helical stacks [10–12].

The detailed structure of such models critically depends on the geometry of the DNA beyond its direct contact with the histone octamer. An experimental pyrimidine dimerization study suggested that the linker DNA is straight [13]. Linking number data suggest that the linker DNA arms do not cross [14] and cryo-electron microscopy micrographs show a zigzag motif of the linker DNA in the compacted fiber [15]. Further support for the two-start zigzag model comes from an analysis of radiation-induced *in vivo* fragmentation of chromatin [16]. Dorigo et al. [17] analyzed *in vitro* compacted dodecamer nucleosome arrays stabilized by introduction of disulfide cross-links between the tails of H4 and H2A histones at the stacking internucleosomal surfaces, and could show that the chromatin fiber comprises two stacks of nucleosomes in accord with the two-start model. The crystal structure of a compact tetranucleosome shows that the linker DNA zigzags back and forth between two stacks of nucleosome cores forming a truncated two-start helix [18]. By successively stacking these tetranucleosome structures one on another, continuous crossed-linker fiber models can be built. The linker DNA is extended with one linker being straight and the other showing a moderate bend. Most probably, the length of the linker DNA is buffered by stretching of the DNA contained in the nucleosome cores. These experimental results favor two-start over one-start models and suggest that the linker DNA may be rather straight, findings supported by theoretical chromatin modeling studies [19–22]; for a review see [23]. In the modeled 30-nm fiber structures, the linker DNA remains extended and passes through the center of the fiber; the structures differ in the amount of nucleosome stacking in the condensed fiber.

Obviously, the forces modulating fiber condensation are mainly electrostatic [20, 24] and thus can be biochemically regulated by phosphorylation, acetylation, and other post-transcriptional modifications that are known to be associated with various genetic pathways. Furthermore, nucleosomes interact with one another. Part of the histone H4 tail (amino acids 14–19) is necessary for fiber compaction [25]. This region makes an interparticle contact with H2A/H2B of a neighboring particle [4, 17, 26]. This internucleosomal interaction was also considered in the chromatin Monte Carlo model by Wedemann and Langowski [21]. However, fiber packaging critically depends on the connecting DNA; the chromatin fiber properties result from the interplay between linker DNA stiffness,

electrostatics, and internucleosomal interactions. Double-helical DNA is a polyelectrolyte with well-defined stiffness (persistence length of 150–190 bp). Length variations are coupled with an axis increase of 0.34 nm and a twist angle of roughly 36° per bp. In particular for short linker lengths, only limited sets of linker lengths can sterically be realized in compacted chromatin fibers, other linker lengths will result in nucleosome clashes. Indeed, analyzing a large number of nucleosome repeat lengths, values related by multiples of the helical twist of DNA were found to be preferred [27]. This implies that specific linker lengths are indeed favored in naturally occurring chromatin fibers.

Here we analyzed the steric stability of rigid assembly fiber structures constructed from nucleosomes and straight linker DNA at atomic resolution for repeat lengths ranging from 155 to 211 bp. This analysis gives first indications about which nucleosome repeats are sterically excluded by assuming a completely rigid linker DNA. In a second step, we introduce DNA flexibility and thermal fluctuations on the modeled chromatin structures by using a Monte Carlo model containing the full energetics of DNA bending and twisting as well as DNA–DNA and nucleosome–nucleosome interactions. While the Monte–Carlo model predicts a larger region of acceptable nucleosomal repeats, both approaches consistently show stable repeats with a period of one DNA helical turn.

2 Methods

To study structural properties and stability of the 30-nm chromatin fiber for different repeat lengths, we compared rigidly assembled chromatin fibers at atomic resolution with modeled chromatin fibers equilibrated by a Metropolis–Monte Carlo algorithm.

2.1 Rigid assembly models of the chromatin fiber

The rigid assembly of the chromatin fiber starts with the crystal structure of a single nucleosome core particle ([4]; PDB code: 1aoi). In the first step, straight linker DNA of a defined length is attached to the DNA leaving the nucleosome. The linker DNA consists of two additional base pairs (bp) at each end. These two base pairs are superimposed to the last two base pairs at one end of the nucleosome core particle DNA. Then, another nucleosome is connected in the same manner to the other end of the linker DNA. By iterating this procedure, we constructed chromatin fibers consisting of 24 nucleosomes connected by 23 linkers and DNA linker lengths in the range of 9–65 bp corresponding to nucleosome repeat lengths between 155 and 211 bp. For model building, InsightII was used (Accelrys, San Diego, USA). We analyzed the relative geometrical orientation of

nucleosomes and the total length and diameter of the models as well as a possible steric hindrance. Steric hindrance analysis was performed using the BUMP command available in InsightII, which will signal van-der-Waals overlaps within the structures. Model structures without bumps are classified as “stable”, all other structures as “unstable”. The end-to-end distances of the 24-nucleosome structure were determined by measuring the distances between the O5' atoms of the first nucleotide in chain I of nucleosomes 1 and those of nucleosomes 22, 23 and 24 (selecting the largest of the three values). The model structure diameters were determined manually on the computer screen by drawing a circle through the outer atoms of a top view orientation and measuring the circle diameter.

2.2 Monte Carlo simulation of the chromatin fiber

Rigid fiber models do not consider the thermal fluctuation that chromatin fibers are subjected to in their natural environment. To study the influence of thermal fluctuation on the fiber stability, we simulated thermodynamic equilibrium ensembles using our Monte Carlo (MC) model, which has been described in earlier work [21, 28]. A statistically relevant set of conformations generated by this method represents the chromatin fiber at thermodynamic equilibrium at a defined temperature. To separate these structures into stable and unstable fibers, we analyze them qualitatively by visualization and quantitatively by determining their fundamental structural parameters such as the contour length, the mass density, and the total internal energy of the chain. We compare the stable and unstable regions thus obtained with that of the rigid assembly models of chromatin fibers.

The Monte Carlo model approximates the chromatin fiber as a flexible polymer chain. The nucleosome shape is represented by a rigid ellipsoidal disk with a diameter of 11 nm and a height of 5.5 nm, approximating the crystal structure [4, 26]. The nucleosome disks are connected via two cylindrical segments corresponding to the linker DNA, in agreement with the tetranucleosome crystal structure [18]. The global shape of the fiber is determined by four parameters: the linker-DNA length l , the linker-DNA opening angle α , the twisting angle β between consecutive nucleosomes, and the attachment angle δ , i.e., the angle between the attachment points of the linker DNA to the nucleosome core (Fig. 1). This geometry is essentially the “two angle” geometry proposed originally by Woodcock et al. [11] and van Holde and Zlatanova [29]. The length of the linker DNA is varied in the range of 9–65 bp. The rigid assembly models and the crystal structure of the tetranucleosome by Schalch et al. [18] show a twist angle $\beta \approx 72^\circ$ for a linker length $l = 20$ bp. Linker length l and

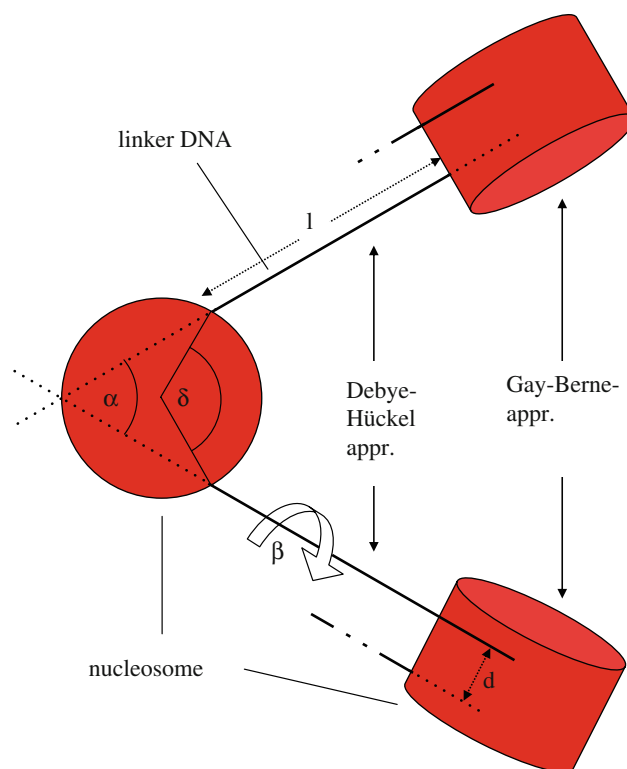


Fig. 1 The geometry of the Monte-Carlo fiber model. Incoming and outgoing linker DNA of length l define the opening angle α and are set a distance d off each other. The attachment points of the linker DNA to the nucleosome are symmetrical and defined by the angle δ . Succeeding nucleosomes are twisted by the torsion angle β . Interactions between the linker segments are described by a Debye-Hückel-Potential whereas nucleosomes interact via a Gay-Berne-Potential [21]

twisting angle β depend on each other through the helical pitch, which was taken here as 10 bp for simplicity and for comparison to the rigid assembly models:

$$\beta = (\text{linker length } l - 20 \text{ bp}) \cdot 36^\circ + 72^\circ$$

The opening angle α between incoming and outgoing linker DNA is set to 60° , which is in the range of 55° and 65° extracted from the crystal structures [18] and the rigid assembly models. In agreement with the crystal structure, incoming and outgoing linker DNA are set 3.1 nm apart, parallel to the superhelical axis of the nucleosome. As 147 bp of DNA is wrapped around the histone core 1.67 times, the separating angle δ is set to $360 - (360 \times 0.67) = 118.8^\circ \approx 119^\circ$, assuming that the linker DNA leaves and enters symmetrically. For comparison, we performed additional simulations with $\alpha = 0^\circ$ and $\delta = 180^\circ$.

Stretching and torsion potentials connecting the linker DNA segments with each other and the nucleosomes are assumed to be harmonic. A screened Coulomb potential in the Debye-Hückel approximation is used to model

electrostatic DNA–DNA interaction, while a weakly attractive anisotropic Lennard–Jones type (Gay–Berne-) potential describes the nucleosome–nucleosome interaction. These potentials are the same as in our previous publications [21, 28]. Electrostatic effects were not explicitly considered in the nucleosome–nucleosome interactions, because the effect of salt on internucleosomal interactions is not well understood.

2.3 The simulation protocol

The simulation is based on two different Monte Carlo steps: a rotation and a pivot move. In the rotation move, the end point of a randomly chosen segment is rotated by a random angle around the axis determined by the start point of the chosen segment and the end point of the next segment. For the pivot move, the shorter part of the chain is rotated by a random angle around a random axis passing through a randomly selected segment point. For comparability with the data of the rigid assembly model fiber structures, we used fibers consisting of 24 nucleosomes and the same values for linker lengths and torsion angles. To check for any dependence on the number of nucleosomes, we also simulated fibers consisting of 100 nucleosomes. The initial parameters of the simulation are given in Table 1.

Two energetically different starting conformations were used to ensure the independence of our simulations from the starting conformation. One simulation run was initialized with a condensed fiber in a twisted zigzag form, where the sum of elastic energies was zero (Fig. 2a). In the second simulation run, all segments were ordered in a straight line, building a linear starting conformation (Fig. 2b). To define the contour of a 30-nm chromatin fiber, we

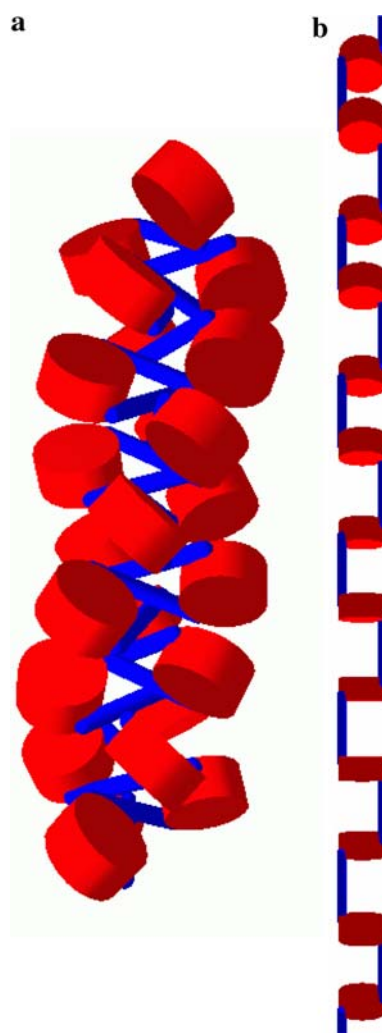


Fig. 2 Twisted (a) and linear (b) initial conformations for simulation of fibers consisting of 24 nucleosomes (red), linker segments (blue) of repeat length $l = 192$ bp, opening angle $\alpha = 60^\circ$, twisting angle $\beta = 288^\circ$ and attachment angle $\delta = 119^\circ$

Table 1 Elastic, interaction and geometric parameters used in the MC simulations (taken from [28])

Parameter	Measure
Stretching modulus DNA	1,104 pN
Bending modulus DNA	2.06×10^{-19} J nm
Torsion modulus DNA	2.67×10^{-19} J nm
Electrostatic radius DNA	1.2 nm
Stretching modulus nucleosome	1,104 pN
Torsion modulus nucleosome	1.30×10^{-19} J nm
Gay–Berne parameters for internucleosome interaction	$\sigma_0 = 10.3$ nm $\chi = -0.506$ $\chi' = -0.383$
Temperature	20°C
Nucleosome diameter	11 nm
Nucleosome height	5.5 nm
Salt concentration	0.1 M NaCl

calculated the mass centers of all stretches of 14 consecutive nucleosomes along the fiber structure. The connected centers of mass form a segmented chain whose sum of segment lengths is a measure of the contour length of the central 86 nucleosomes of the fiber. For calculating the persistence length and stretching modulus of this chain, we used the analysis methods given in our previous paper [28]. To check the statistics of our simulations, we calculated the autocorrelation function of the energy, mass density, end-to-end distance, and contour length as described there and found correlation lengths less than 3,500 MC steps which is in the range of our former simulations. We performed 3×10^6 MC steps for each simulation where the first 5.10^5 MC steps (corresponding to more than 100 statistically independent conformations) were used only for the initial relaxation of the chain and not included in the analysis. For the final analysis, every 1,000th conformation of the

remaining 2.5×10^6 has been included. Total energy, contour length, end-to-end distance, and mass density of the fiber after the equilibration in concord for both starting conformations (data not shown).

3 Results

To study the structure and stability of the 30-nm chromatin fiber and the dependence of its physical parameters on the underlying geometry of the zigzag chain, we first constructed and analyzed rigid assembly models for eventual steric clashes. We then performed MC simulations with nucleosomal repeats between 156 and 211 bp and compared thermodynamically equilibrated fiber structures with the rigid assembly models, which are based on the crystal structure of the nucleosome and B-form linear DNA for the linker DNA. In MC simulation setup 1 (Fig. 3a), the linker attachment points were set a maximum distance apart from each other ($\delta = 180^\circ$) while incoming and outgoing linker-DNA are parallel ($\alpha = 0^\circ$). In MC simulation setup 2 (Fig. 3b), bending angle $\alpha = 60^\circ$ and attachment angle $\delta = 119^\circ = 360 - (1.67 \times 360) \bmod 360$ were chosen according to the geometric models and the tetranucleosome structure [18].

3.1 Rigid assembly structures

We constructed rigid assembly models from experimental nucleosome structures and straight linkers for linker lengths between 9 and 65 bp corresponding to repeat

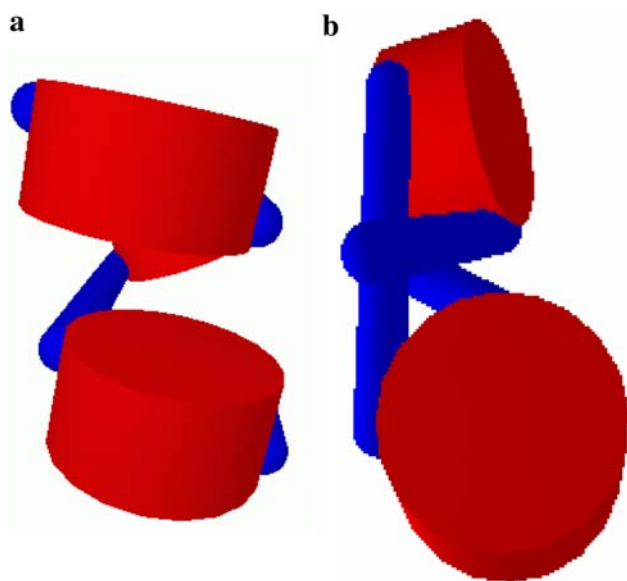


Fig. 3 Visualization of the local geometry of our model for simulation setup1 with opening angle $\alpha = 0^\circ$ and attachment angle $\delta = 180^\circ$ (a) and simulation setup 2 with $\alpha = 60^\circ$ and $\delta = 119^\circ$ (b)

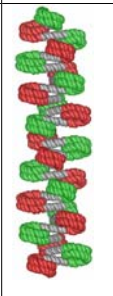

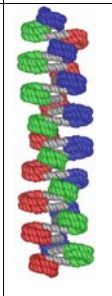

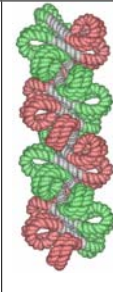
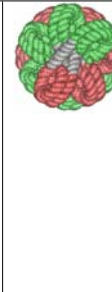

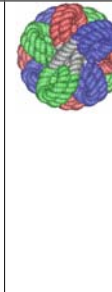
lengths between 155 and 211 bp. Rigid assembly of nucleosomes and straight linkers leads to relatively crude models that take into account neither specific nucleosome–nucleosome interactions nor a potential bending of the DNA linkers. Nevertheless, the structural features shown by these models are a solid basis for more sophisticated analyses.

We analyzed possible steric hindrances in these models and found that structures with linker lengths 9–13, 20–24, 32–36, 43, 46, and 56 bp show bumps. A full comparison of all these structures is given in Table 1 of the Supplementary material. In some cases, the number of bumps is relatively small and could easily be removed by a slight geometrical adjustment. The rigid assembly models exhibit structural regularities that are governed by the varying linker lengths. The relevant geometrical parameters are the end-to-end-distances of the linkers and the torsion angles between the nucleosomes at the two linker ends. The latter angles are governed by the helical twist of about 36° for ideal B-DNA. Of course, steric hindrance becomes smaller and smaller with increasing linker lengths. Concurrently, the structures switch between two-start models with a preferred interaction between nucleosomes n and $n + 2$ and three-start models with a dominant $n/n + 3$ nucleosome interaction. However, for shorter linker lengths, most of the two-start structures are sterically forbidden. Two representative examples of a two-start and a three-start structure with linker lengths 31 and 27 bp are shown in Fig. 4 (A compilation of more top and side views in a two-start and a three-start coloring scheme is shown in Supplementary Fig. 1). The rigid assembly models allow also an easy determination of end-to-end distances and diameters of the chromatin structures (Fig. 5). The chromatin model diameter increases from 19.6 nm for a linker length of 9 bp to 41.3 nm for a 65-bp linker. Superimposed to this general increase is an oscillating behavior with maxima at 25/26, 36/37, 46/47, and 57 bp and minima at 29/30, 39–41, 50/51 and 61 bp. The end-to-end distances also exhibit an oscillating behavior around a constant value up to about 35 bp and then start to increase.

3.2 Stable and unstable fibers in the MC simulations

Rigid assembly models are assumed to be stable if they have no bumps (Table 1, supplement). To decide whether the simulated fibers were stable or unstable for the thermodynamically equilibrated MC models, we first studied them qualitatively by eye. Stable fibers have a very regular structure (Fig. 6a), while unstable fibers are characterized by a lumpy structure and aggregated nucleosomes (Fig. 6b). We analyzed the fibers quantitatively by comparing characteristic parameters such as energy, mass density, contour length, and end-to-end distance. Plotted as

Fig. 4 Rigid assembly models with linker lengths 27 and 31 bp (two-start coloring: nucleosomes n - red, nucleosomes $n + 1$ green; three-start coloring: nucleosomes n - red, nucleosomes $n + 1$ - green, nucleosomes $n + 2$ - blue)

Linker Length (bp)	Repeat Length (bp)	2-start coloring (side view)	2-start coloring (top view)	3-start coloring (side view)	3-start coloring (top view)
27	173				
31	177				

a function of the repeat length (Fig. 7), all parameters show a periodic behavior with a period corresponding to the helical pitch of the linker-DNA of 10 bp.

For simulation setup 1 (Fig. 7a), there are peaks located at repeat lengths 160–210 bp in steps of 10 bp. They represent unstable fibers, characterized by a high total energy and mass density and a correspondingly low contour length and end-to-end distance. The nucleosomes are aggregated into lumpy structures (Fig. 6b). Fibers with repeat lengths shorter than 160 bp were unstable due to strong interactions between the nucleosomes. Stable fibers with the highest compaction have repeat lengths between 161 and 211 in steps of 10 bp. In comparison to the rigid assembly models, more of the MC-generated structures are stable (Fig. 7c) as thermal fluctuations allow avoiding collisions, which is not possible in static structures.

The results of simulation setup 2 (Fig. 7b) show the impact of changes in the local geometry. The peak positions are shifted 1 or 2 bp to higher repeat lengths. Similar to setup 1, unstable fibers are located at an interval of 10 bp for repeat lengths smaller than 193 bp. For repeat lengths higher than 192 bp, the thermal fluctuations allow the fiber to avoid aggregation and no unstable conformations were found anymore. The characteristic fluctuation of the energy, contour length, end-to-end distance, and mass density parameter is still preserved. The rigid assembly models also show less unstable conformations for longer linkers. Unstable fibers in the MC model occur around the

same linker lengths as for the rigid assembly structures, although there are less of them and the structures are less regular due to thermal fluctuation. The points corresponding to the most stable fibers are located between 163 and 212 bp in steps of 10 bp, thus 2 bp higher than for setup 1.

Simulated 100-nucleosome fibers exhibit the same variation in stability with repeat length as those consisting of 24 nucleosomes. Peak positions and periodical behavior for energy, mass density, contour length, and end-to-end distance for fibers are also identical for these two lengths (data not shown). By increasing the attachment angle δ in simulation setup 2 from 119° to 126° , which corresponds to an earlier nucleosome crystal structure [4, 26], we found that the repeat lengths of unstable and stable fibers remain unchanged.

3.3 N-start fibers

To characterize the fibers further, we analyzed their helical structure. It is easily seen that in an n -start fiber the mean distance between two nucleosomes will be minimal if they are separated by $n-1$ nucleosomes. The classical solenoid model for the 30-nm chromatin, in which the nucleosomes follow a helical path, is a typical one-start model, as the minimal distance occurs for consecutive nucleosomes. On the other hand, the original zig-zag model by Woodcock et al. [11] is an example of a two-start helix, as is the X-ray structure of the tetranucleosome by Schalch et al. [18]. In

Fig. 5 *Upper panel* dependence of the chromatin fiber diameter on linker length according to the type I model. The diameter was determined from a circle passing through the projections of outer atoms onto a plane perpendicular to the long fiber axis. *Lower panel* dependence of the end-to-end distance of the 24-nucleosome chromatin models on linker length

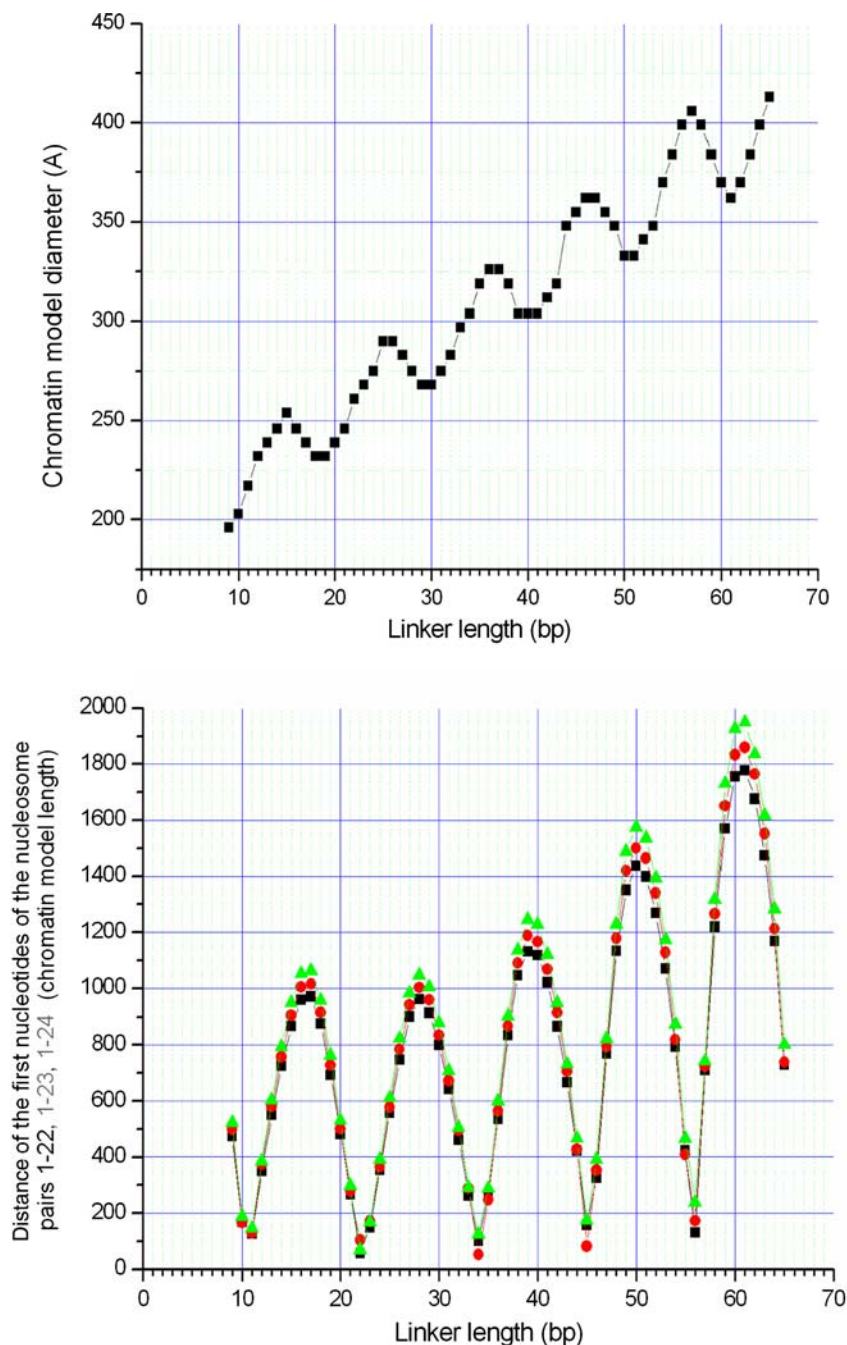


Fig. 4, the rigid assembly model structures are shown in a one-start, two-start, and three-start coloring mode. These coloring schemes allow an easy classification of individual models.

Figure 8 shows typical mean distance distributions from which we determine the type of the nucleosome helix in the Monte Carlo models. Typical conformations for one-, two-, and three-start structures are presented in Fig. 9.

The data for simulation setup 1 (Fig. 10) are dominated by one-start fibers at short repeat lengths, whereas the number of two-start fibers increases for higher repeat

lengths. In particular, fibers with high mass density have a two-start structure and are located in the range of 170 ± 2 bp with a period of 10 bp. No three-start models or higher were found for this parameter setup.

For simulation setup, two more two-start fibers are observed, located at repeat lengths 161 ± 1 bp in steps of 10 bp for a repeat length smaller than 176 bp, and otherwise at 180 ± 1 bp in steps of 10 bp. Three-start models occur for repeat lengths higher than 181 bp in the range of 182 ± 1 bp with a period of 10 bp and mainly for fibers with higher mass density. However, not all of these fibers

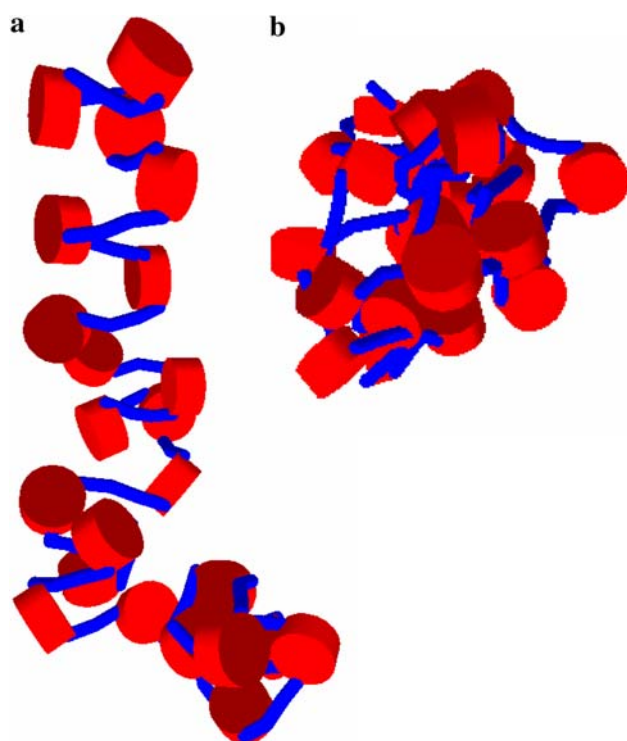


Fig. 6 Typical stable (a) and unstable (b) structure. Nucleosomes of unstable structures aggregate and form clumps

are stable. Similar three-start fibers have been found in the rigid assembly models.

Simulations with a higher opening angle $\delta = 126^\circ$ show similar results as in simulation setup 2. However, the total number of one-start structures is slightly higher, and two- and three-start structures are sometimes shifted by 1 bp.

3.4 Influence of the attachment angle δ

Finally, we investigated the influence of the position of the linker DNA attachment points on the structural parameters of the 30-nm chromatin fiber. To accomplish this aim, we varied systematically the attachment δ of the linker DNA. This is important for further development of the model, for example, to include nucleosome unwrapping. The simulations use setup 2, which is based on the crystal structure of the tetranucleosome [18]. The repeat length of the chromatin fiber is 167 bp. 147 bp of the DNA are wrapped 1.67 times around one nucleosome leading to an opening angle of 119° . The simulated fibers consist of 100 nucleosomes.

In the first simulation series, the length of the linker DNA was kept constant and the opening angle was varied systematically (Fig. 11). If the attachment points of the linker DNA are farther apart (corresponding to a high opening angle), the structures are more open. This becomes apparent in the 40% increase of the contour length and the

end-to-end distance of the fiber with increasing opening angle. Accordingly, the mass density drops by roughly 40%.

The opening angle α of the linker DNA decreases as the attachment points are moved apart. Here the change is about 20%. Such a behavior can be expected, as the electrostatic repulsion of the linker DNA segments, which dominates the opening angle, depends on the mutual distance. At first, the persistence length of the fiber is slightly decreasing, but for the biologically interesting region of $\delta > 50^\circ$, we find an increase of about 30%. On the other hand, the stretching modulus in this region decreases about 30% and the fiber is easier to stretch.

We then studied the effect of unrolling DNA from the nucleosomes at a fixed repeat length of 167 bp. This takes into account that the length of the linker DNA depends on the extent of unwrapping (Fig. 12). The torsion angle β is kept constant because the repeat length remains unchanged.

Similar to the previous simulation series with the fixed linker length, the fiber structure is more open for larger attachment angles. This is seen by the increase in the contour length of 30% and the decrease in mass density of 20%. Also, the linker opening angle increases by 30%, which is not the case in the simulation with fixed linker length. This increase seems to be caused mainly by the stronger repulsion of the longer linker DNA for higher opening angles.

Remarkable is the trend of the end-to-end distance, which varies in contrast to the contour length by only about 3%. Thus, open fibers with a high distance between the linker DNA attachment points are more flexible. This is supported by the corresponding changes in persistence length and stretch modulus, which decrease by 50 and 90% respectively, for increasing opening angle.

As thermal fluctuations can change the DNA bound to the nucleosome only by a few bp, we finally analyzed the fiber structures with an attachment angle $\delta = 89^\circ$ – 139° corresponding to 147 ± 5 bp of DNA bound to the nucleosome. Even in this small interval, contour length and mass density are still changing by about 10 and 7%, respectively. The end-to-end distance remains nearly constant and changes by only about 1%. Persistence length and stretching modulus show a decreasing trend of 20 and 40%, respectively. Thus, the desorption of a few base pairs in our simulations already leads to a significant increase in fiber flexibility.

4 Discussion

Due to its fundamental importance, strong efforts, using both experimental and model-building approaches, have been put into the elucidation of the chromatin fiber

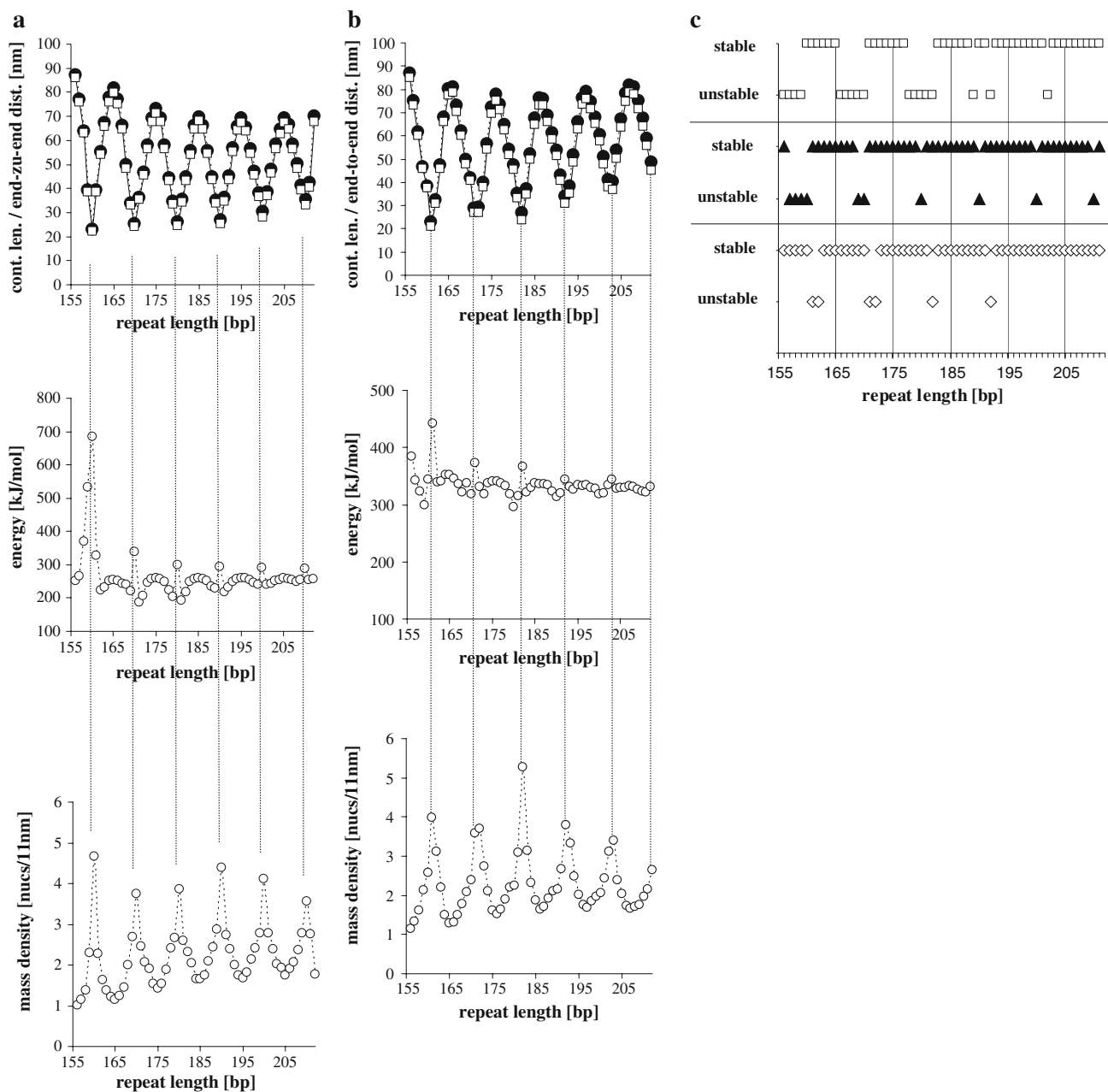


Fig. 7 **a** Contour length (*closed circles*), end-to-end distance (*open squares*), energy and mass density as function of the repeat length for $\alpha = 0^\circ$ and $\delta = 180^\circ$. All plots show peaks for conformations with repeat lengths of 160–210 at a period of the helical pitch of 10 bp. These unstable structures are characterized by a low contour length and end-to-end distance but high energy and mass density. **b** Contour length (*closed circles*), end-to-end distance (*open squares*), energy and mass density as function of the repeat length for $\alpha = 60^\circ$ and $\delta = 119^\circ$. The peaks are shifted by 1–2 bp compared to simulation setup 1 due to the different local geometry whereas the period of

10 bp remains the same **c** Stable and unstable structures found in the rigid assembly model and the simulation. As a result of the thermal fluctuations, there are less unstable fibers than predicted by the rigid assembly models. For higher repeat lengths the number of collisions and as a result the amount of unstable conformations decreases. Unstable structures in the simulations as well as in the rigid assembly models occur with a period of 10 bp. *open squares* rigid assembly model; *closed triangles* Monte Carlo model, parameter setup 1, $\delta = 180^\circ$, $\alpha = 0^\circ$; *open diamonds* Monte Carlo model, parameter setup 2, $\delta = 119^\circ$, $\alpha = 60^\circ$

structure. On the experimental side, in particular X-ray crystallography for mono- and oligonucleosomes and electron and atomic force microscopy for higher order structures, but also chemical cross-linking and nuclease

digestion have contributed tremendously to our understanding of this complex and its fundamental biopolymer structure. There is a plethora of different models trying to unite all these experimental data to a unified view of the

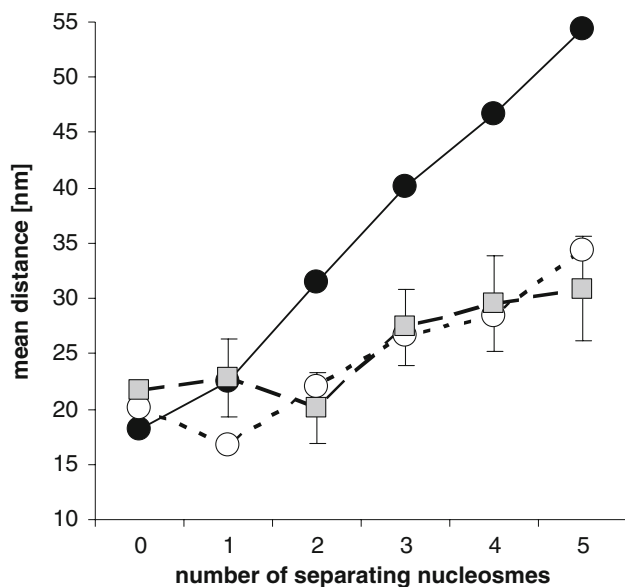


Fig. 8 Mean distance distributions of nucleosomes for simulated fibers showing a typical one-, two- or three-start structure. The position of the minima defines the starting structure. *Closed circle* $l = 187$ bp, $\alpha = 60^\circ$, $\delta = 119^\circ$; one-start fiber *open circle* $l = 190$ bp, $\alpha = 60^\circ$, $\delta = 119^\circ$, two-start fiber; *squares* $l = 192$ bp, $\alpha = 60^\circ$, $\delta = 119^\circ$, three-start fiber

chromatin fiber structure. In the seminal review by van Holde and Zlatanova [29], the time period between 1980 and 1986 has been featured as an ‘orgy of model building’. Most of these models fall into two classes: the one-start solenoidal helix with a coiled linear array of nucleosomes and the two-start helix with a zigzag path of nucleosomes. These models differ in a number of geometric features. For example, for the solenoidal helix the fiber diameter should, at first approximation, not depend on the linker length, while it does so in the two-start helix model. It is important to realize that none of these models has been worked out at atomic detail, but is rather described in terms of overall helical parameters. Recently, Schalch et al. [18] have taken a first step toward the atomic-detail resolution of the chromatin fiber structure by solving the X-ray structure of a tetranucleosome array. This structure is in favor of a two-start helix.

Here, we describe atomic-detail models of the chromatin fiber structure for linker lengths between 9 and 65 base pairs and 24 nucleosomes, generated by assembling successively nucleosomes and stretches of B-DNA. A drawback of these models is the assumption of straight linkers. In the two-start-helix model, the linkers are rather straight; however, bending may occur due to interactions of the histone tails of the linker histone with the DNA. As very little is known about the detailed structure of the H1-DNA complex, the role of the linker histone H1 can be taken into account only approximately by shifting the point

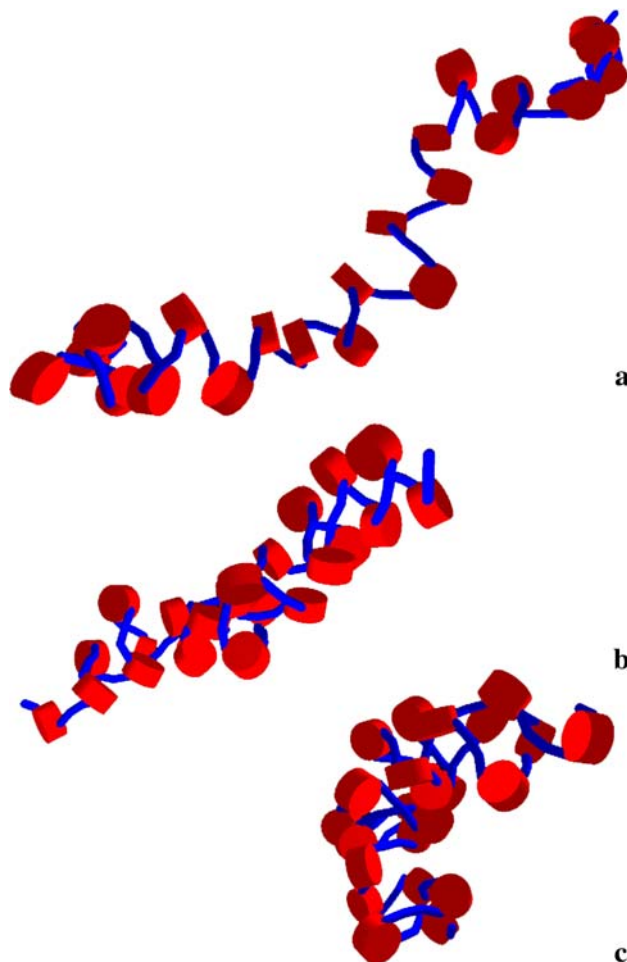


Fig. 9 Typical fiber conformations, which are classified as one-start (a), two-start (b) and three-start (c) structures based on the mean distance distribution of their nucleosomes

of attachment of the DNA on the nucleosome core. Here we used these models to study the effect of linker length on possible regions of stability for chromatin fibers and to compare the atomic-detail rigid assembly models with straight linkers with the Monte-Carlo model structures that do not give atomic detail but relax the straightness assumption.

Increasing the linker length from 9 to 65 bp, we find that both models agree on those nucleosome repeats that are forbidden for stable fiber structures, with the exception that the thermal fluctuations in the MC model relax the steric requirements to some extent. We do not find any indication of a one-start helix. It is noteworthy, though, that in some cases a three-start helix seems to be the most appropriate description of the resulting structure. One earlier proposal of such a three-start structure was made by Makarov et al. [19].

As shown in Fig. 5, the fiber diameter depends on linker length, showing an oscillatory behavior. Some experimental observations confirm this phenomenon, for

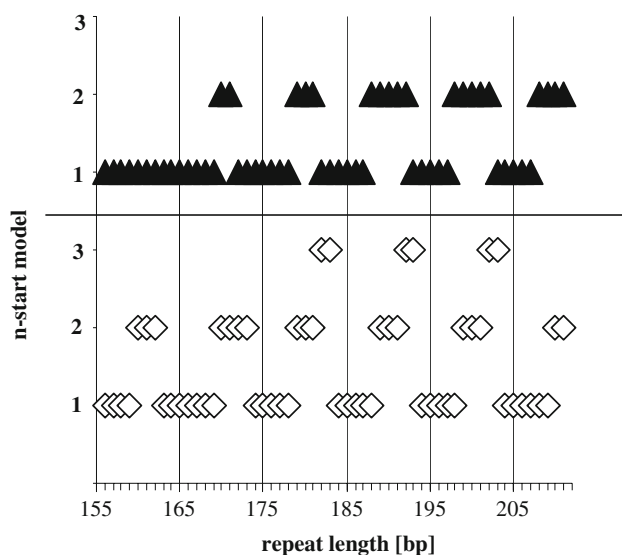


Fig. 10 Overview of the n -start fibers for simulation setup 1 with $\alpha = 0^\circ$ and $\delta = 180^\circ$ and simulation setup 2 with $\alpha = 60^\circ$ and $\delta = 119^\circ$. For high repeat lengths the number of one-start structures is decreasing. In simulation setup 2 are fewer one-start structures than in simulation setup 1. Further we found three-start structures for repeat length higher than 180 bp in simulation setup 2, but most of them are unstable. Similar three-start structures have also been observed in the rigid assembly model. Closed triangles parameter setup 1, $\delta = 180^\circ$, $\alpha = 0^\circ$; open diamonds: parameter setup 2, $\delta = 119^\circ$, $\alpha = 60^\circ$

instance, the recent electron microscopy data by Robinson et al. [30] that show a jump in fiber diameter with nucleosome repeat. Of course, also the end-to-end distances of the model structures are dependent on linker length: they are relatively constant for short linkers up to about 35 bp but then start to increase. Due to the strong ‘lumping’ for the unstable nucleosome repeats, the dependence of the end-to-end distances on linker length oscillates very strongly.

In agreement with rigid assembly chromatin fiber models, we found unstable fibers in thermodynamic equilibrium at particular repeat lengths. They occurred with a repeat length periodicity of 10 bp, which corresponds to the helical pitch of DNA. The same periodicity is separating the most densely compacted fibers from each other. This explains the fact that certain repeat lengths are preferentially found in organisms. A quantization of the repeat length is also observed by experimental data: Gel bands from the analysis of single-stranded DNA of dinucleosomes were separated by multiples of ≈ 10 bp [31]. Other experiments in which chromatin was digested by DNase I and DNase II found two sets of bands with a period of ≈ 10 bp shifted by 5 bp against each other [32–34]. A similar study could not confirm this $(10n + 5)$ base pair cleavage pattern, but found a quantization with a shift of -1 to -3 bp [35]. Other studies could not observe any shift

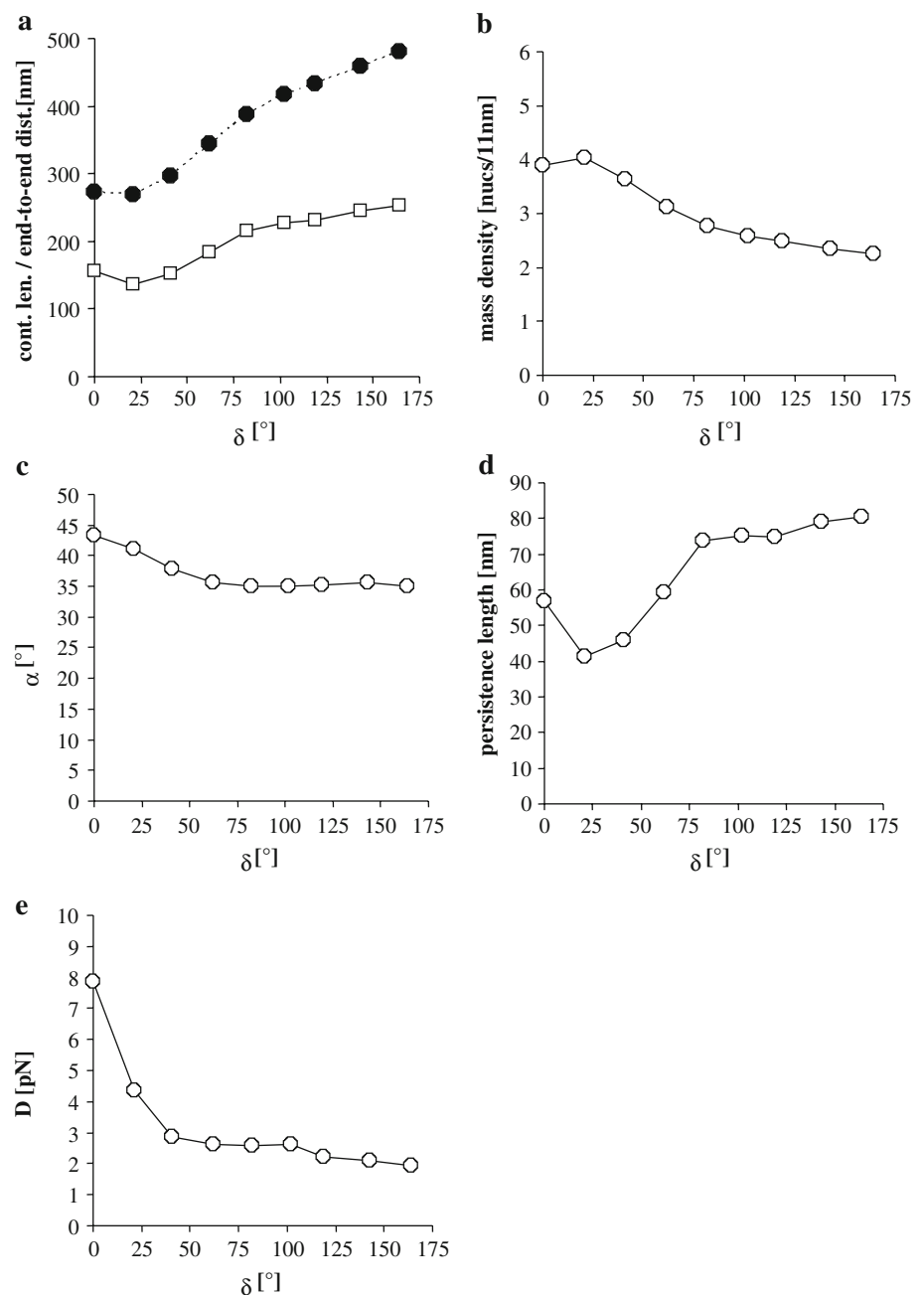
[36–38]. This, however, is not in contradiction to the quantization of repeat lengths, as in these experiments, the restriction enzymes cut the DNA non-specifically and not at the entry and exit points of the nucleosomes. More specific restriction experiments cleaved the DNA ends of dinucleosomes precisely using exonuclease II and S1 nuclease [34]. The observed band of the single-stranded DNA products showed shoulders at intervals of 10 bp, which is in agreement with the repeat length period found in our simulations.

The quantization we observed in our simulations is in good agreement with the results of Widom [27]. By summarizing the outcome of different experiments, which determined the repeat length of different organisms, and analyzing them systematically, he could establish a quantization of the repeat length with a period of 10 bp. Rigid assembly models fail to explain the quantization observed for long repeat length, as no steric collisions exist anymore. On the other hand, for all parameter sets, the Monte Carlo simulations showed that depending on the repeat length the local geometry leads periodically to fibers of higher and lower compaction. This influence is still present for long repeat lengths. The points of highest compaction are located next to the unstable fibers, which we found at repeat lengths of 162, 172, 182, 192, and 202 bp. These are in agreement with the probability distributions of Widom [27], which show local minima at 162, 172, 182, 193, and 202 bp repeat lengths. Considering the fact that a high compaction is advantageous for an organism, these repeat lengths should be more frequently found in nature than in others and therefore could explain the quantization.

Of course, the repeat length period adopts an exact value of 10 bp only in our model. Widom [27] gives a value, depending on the data sets he used and their errors, of 9.0 and 10.5 bp. In particular for high repeat lengths, there exist only a few measurements and as a result, the maxima in the probability distribution of the repeat length is flat. Identification and elimination of incorrect measurements may lead to a more precise measurement of the periodicity. Furthermore, there are genomic constraints that can lead to a deviation from the preferred repeat length, for example, proteins, which play an important role in transcription and replication or special DNA sequences, thus resulting in a preferred nucleosome positioning.

In agreement with the rigid assembly fiber models, we found in the MC simulations mainly one- and two-start fibers, but surprisingly also some three-start fibers [19]. The two-start fibers occur at repeat lengths with a high mass density and show an irregular zig-zag structure with nearly straight linker DNA, in agreement with the model given in [11]. In our simulations, one-start structures are elongated fibers with a low compaction. Due to their nearly straight linker DNA, they resemble the zig-zag model

Fig. 11 Contour length and end-to-end distance (a), mass density (b), opening angle (c), persistence length (d) and stretching modulus (e) as a function of the attachment angle δ for constant linker DNA length of 21 bp. Increasing counter length, end-to-end distance and decreasing mass density show that an increasing δ leads to an opening of the fiber. A higher distance between the linker DNA for higher δ leads to a decrease in opening angle. In the biological interesting range of $\delta > 50^\circ$ the stretching stiffness increases, whereas the stretching stiffness is decreasing. *Filled circles* contour length; *open squares* end-to-end distance



more than the solenoid model. Three-start structures are fibers with the highest mass densities; most of them are unstable.

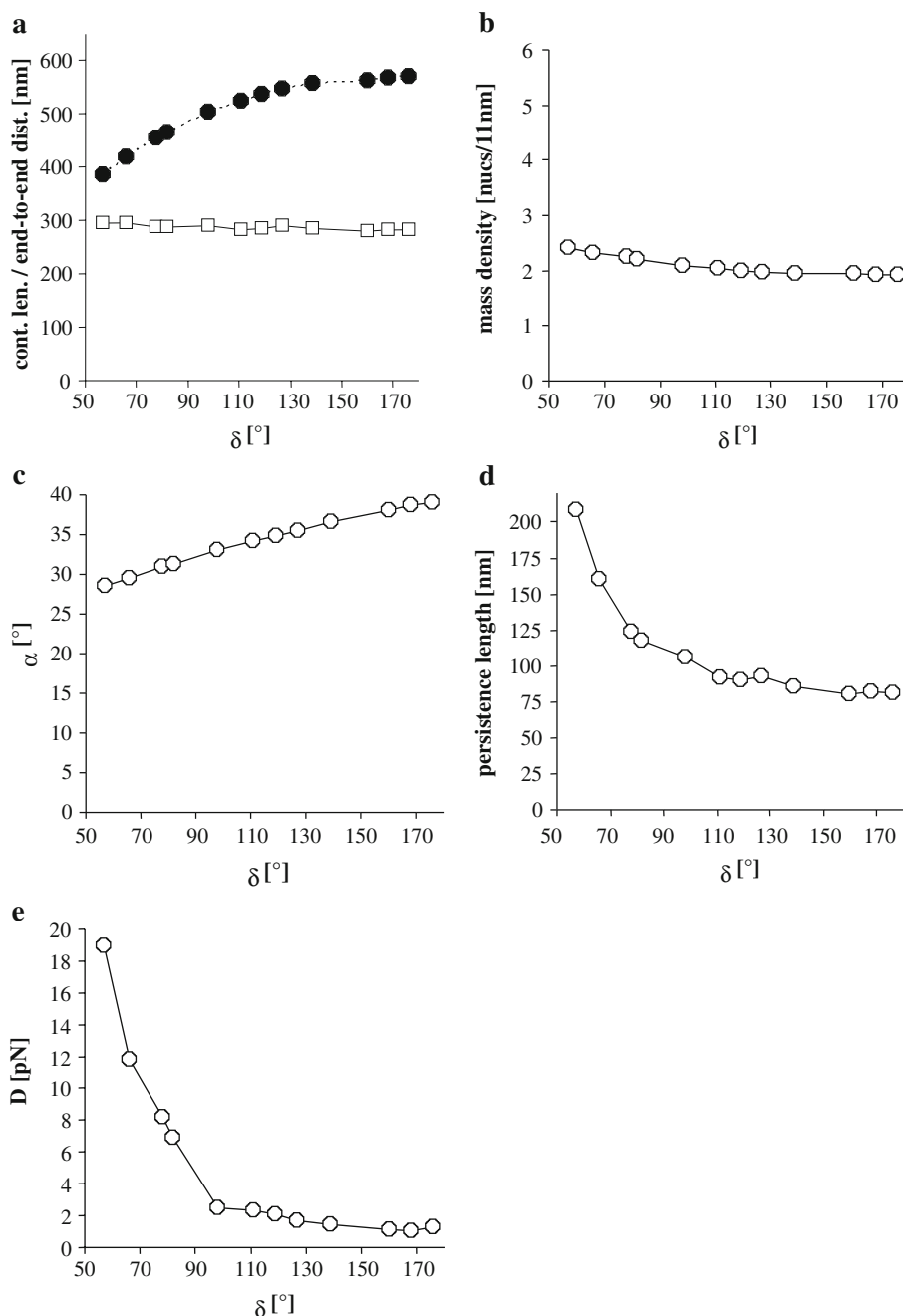
Our results show that the helix topology of the chromatin fiber depends on the repeat length. As the latter may vary by a few base pairs within a chromatin fiber, it is possible that the fiber has different local helical topologies. This could explain the different experiments, which are in favor of either the one-start [6, 7, 29, 39] or the two-start model [11, 15, 40–44].

Systematic variation of the attachment angle δ showed that an increasing distance between the attachment points

of the linker DNA to the nucleosomes leads to more open and flexible fiber structures. Therefore, a local unbinding of the DNA due to thermal fluctuation in one part of the fiber means a considerable facilitation for the local accessibility and remodeling of the chromatin fiber.

Our results show that rigid assembly models are able to discover important structural properties of the chromatin fiber. But for their realistic assessment, it is necessary to accomplish thermodynamic equilibration. Thermal fluctuation allows the evasion of most collisions found in the rigid assembly models so that no unstable fibers would occur in the simulations; thus, the number of unstable

Fig. 12 Contour length and end-to-end distance (a), mass density (b), opening angle (c), persistence length (d) and stretching modulus (e) as a function of the attachment angle δ for constant repeat length of 167 bp. Similar to Fig. 11 we find more open structures for increasing attachment angle δ shown by an increasing contour length and mass density. In contrast to Fig. 11 the opening angles are increasing for higher δ , since a longer linker DNA leads to stronger repulsion between them. Persistence length and stretching module show that an increasing δ leads to more flexible fibers, which is confirmed by the nearly constant end-to-end distance. *Filled circles* contour length; *open squares* end-to-end distance



structures is much lower in the MC simulations than in the rigid assembly models.

For a more realistic model, it is necessary to improve the detailed description of the interactions. In particular, the implementation of a realistic interaction between nucleosomes and the attached linker DNA would improve the simulation of the nucleosome unwrapping and the interpretation of chromatin fiber stretching experiments [45–49]. This particular DNA binding also influences the nucleosome–nucleosome–interaction since an unrolling of

negatively charged linker DNA leads to a higher positive charge of the nucleosome. Further, a realistic potential modeling the influence of the histone tails and histone H1 will provide a deeper insight into the role of chromatin fiber structure and function in transcription and gene regulation. Notwithstanding these issues, simple model systems can also experimentally give important insights into chromatin structure, as witnessed by the recent study of DNA assembly on spherical nanoparticles, where chromatin-like structures were observed [50].

Acknowledgment This work was supported by the initiative of the VW foundation ‘Physics, Chemistry, and Biology with single molecules’.

References

- Olins AL, Olins DE (1974) Spheroid chromatin units (v bodies). *Science* 183:330–332. doi:10.1126/science.183.4122.330
- Kornberg RD (1974) Chromatin structure: a repeating unit of histones and DNA. *Science* 184:868–871. doi:10.1126/science.184.4139.868
- Arents G, Burlingame RW, Wang B-C, Love WE, Moudrianakis EN (1991) The nucleosomal core histone octamer at 3.1 Å resolution: a tripartite protein assembly and a left-handed superhelix. *Proc Natl Acad Sci USA* 88:10148–10152. doi:10.1073/pnas.88.22.10148
- Luger K, Mäder AW, Richmond RK, Sargent DF, Richmond TJ (1997) Crystal structure of the nucleosome core particle at 2.8 Å resolution. *Nature* 389:251–260. doi:10.1038/38444
- van Holde KE (1989) *Chromatin*, Springer, Heidelberg
- Finch JT, Klug A (1976) Solenoidal model for superstructure in chromatin. *Proc Natl Acad Sci USA* 73:1897–1901. doi:10.1073/pnas.73.6.1897
- Thoma F, Koller T, Klug A (1979) Involvement of histone H1 in the organization of the nucleosome and of the salt-dependent superstructures of chromatin. *J Cell Biol* 83:403–427. doi:10.1083/jcb.83.2.403
- McGhee JD, Nickol JM, Felsenfeld G, Rau DC (1983) Higher order structure of chromatin: orientation of nucleosomes within the 30 nm chromatin solenoid is independent of species and spacer length. *Cell* 33:831–841. doi:10.1016/0092-8674(83)90025-9
- Widom J, Klug A (1985) Structure of the 300Å chromatin filament: X-ray diffraction from oriented samples. *Cell* 43:207–213. doi:10.1016/0092-8674(85)90025-X
- Woodcock CL, Frado LL, Rattner JB (1984) The higher-order structure of chromatin: evidence for a helical ribbon arrangement. *J Cell Biol* 99:42–52. doi:10.1083/jcb.99.1.42
- Woodcock CL, Grigoryev SA, Horowitz RA, Whitaker N (1993) A chromatin folding model that incorporates linker variability generates fibers resembling the native structures. *Proc Natl Acad Sci USA* 90:9021–9025. doi:10.1073/pnas.90.19.9021
- van Holde K, Zlatanova J (1996) What determines the folding of the chromatin fiber. *Proc Natl Acad Sci USA* 93:10548–10555. doi:10.1073/pnas.93.20.10548
- Pehrson JR (1995) Probing the conformation of nucleosome linker DNA in situ with pyrimidine dimer formation. *J Biol Chem* 270:22440–22444
- Prunell A (1998) A topological approach to nucleosome structure and dynamics: the linking number paradox and other issues. *Biophys J* 74:2531–2544. doi:10.1016/S0006-3495(98)77961-5
- Bednar J, Horowitz RA, Grigoryev SA, Carruthers LM, Hansen JC, Koster AJ, Woodcock CL (1998) Nucleosomes, linker DNA, and linker histone form a unique structural motif that directs the higher-order folding and compaction of chromatin. *Proc Natl Acad Sci USA* 95:14173–14178. doi:10.1073/pnas.95.24.14173
- Rydberg B, Holley WR, Mian IS, Chatterjee A (1998) Chromatin conformation in living cells: support for a zig-zag model of the 30 nm chromatin fiber. *J Mol Biol* 284:71–84. doi:10.1006/jmbi.1998.2150
- Dorigo B, Schalch T, Kulangara A, Duda S, Schroeder RR, Richmond TJ (2004) Nucleosome arrays reveal the two-start organization of the chromatin fiber. *Science* 306:1571–1573. doi:10.1126/science.1103124
- Schalch T, Duda S, Sargent DF, Richmond TJ (2005) X-ray structure of a tetranucleosome and its implications for the chromatin fibre. *Nature* 436:138–141. doi:10.1038/nature03686
- Makarov V, Dimitrov S, Smirnov V, Pashev I (1985) A triple helix model for the structure of chromatin fiber. *FEBS Lett* 181:357–361. doi:10.1016/0014-5793(85)80292-1
- Beard DA, Schlick T (2001) Computational modeling predicts the structure and dynamics of chromatin fiber. *Structure* 9:105–114. doi:10.1016/S0969-2126(01)00572-X
- Wedemann G, Langowski J (2002) Computer simulation of the 30-nanometer chromatin fiber. *Biophys J* 82:2847–2859. doi:10.1016/S0006-3495(02)75627-0
- Engelhardt M (2007) Choreography for nucleosomes: the conformational freedom of the nucleosomal filament and its limitations. *Nucleic Acids Res* 35:e106. doi:10.1093/nar/gkm560
- Langowski J, Schiessel H (2004) Theory and computational modeling of the 30 nm chromatin fiber. In: Zlatanova J, Leuba SH (eds) *Chromatin structure and dynamics: state-of-the-art*. Elsevier, Amsterdam, pp 397–420
- Beard DA, Schlick T (2001) Modeling salt-mediated electrostatics of macromolecules: the discrete surface charge optimization algorithm and its application to the nucleosome. *Biopolymers* 58:106–115. doi:10.1002/1097-0282(200101)58:1<106::AID-BIP100>3.0.CO;2-#
- Dorigo B, Schalch T, Bystricky K, Richmond TJ (2003) Chromatin fiber folding: requirement for the histone H4N-terminal tail. *J Mol Biol* 327:85–96. doi:10.1016/S0022-2836(03)00025-1
- Davey CA, Sargent DF, Luger K, Maeder AW, Richmond TJ (2002) Solvent mediated interactions in the structure of the nucleosome core particle at 1.9 Å resolution. *J Mol Biol* 319:1097–1113. doi:10.1016/S0022-2836(02)00386-8
- Widom J (1992) A relationship between the helical twist of DNA and the ordered positioning of nucleosomes in all eukaryotic cells. *Proc Natl Acad Sci USA* 89:1095–1099. doi:10.1073/pnas.89.3.1095
- Aumann F, Lankas F, Caudron M, Langowski J (2006) Monte Carlo simulation of chromatin stretching. *Phys Rev E Stat Nonlin Soft Matter Phys* 73:041927. doi:10.1103/PhysRevE.73.041927
- van Holde K, Zlatanova J (1995) Chromatin higher order structure: chasing a mirage? *J Biol Chem* 270:8373–8376. doi:10.1074/jbc.270.15.8373
- Robinson PJ, Fairall L, Huynh VA, Rhodes D (2006) EM measurements define the dimensions of the “30-nm” chromatin fiber: evidence for a compact, interdigitated structure. *Proc Natl Acad Sci USA* 103:6506–6511. doi:10.1073/pnas.0601212103
- Karpov VL, Bavykin SG, Preobrazhenskaya OV, Belyavsky AV, Mirzabekov AD (1982) Alignment of nucleosomes along DNA and organization of spacer DNA in *Drosophila* chromatin. *Nucleic Acids Res* 10:4321–4337. doi:10.1093/nar/10.14.4321
- Lohr D, Van Holde KE (1979) Organization of spacer DNA in chromatin. *Proc Natl Acad Sci USA* 76:6326–6330. doi:10.1073/pnas.76.12.6326
- Lohr D (1986) The salt dependence of chicken and yeast chromatin structure. Effects on internucleosomal organization and relation to active chromatin. *J Biol Chem* 261:9904–9914
- Strauss F, Prunell A (1983) Organization of internucleosomal DNA in rat liver chromatin. *EMBO J* 2:51–56
- Drew HR, Calladine CR (1987) Sequence-specific positioning of core histones on an 860 base-pair DNA. Experiment and theory. *J Mol Biol* 195:143–173. doi:10.1016/0022-2836(87)90333-0
- Hayes JJ, Tullius TD, Wolffe AP (1990) The structure of DNA in a nucleosome. *Proc Natl Acad Sci USA* 87:7405–7409. doi:10.1073/pnas.87.19.7405

37. Bavykin SG, Usachenko SI, Zalensky AO, Mirzabekov AD (1990) Structure of nucleosomes and organization of internucleosomal DNA in chromatin. *J Mol Biol* 212:495–511. doi:[10.1016/0022-2836\(90\)90328-J](https://doi.org/10.1016/0022-2836(90)90328-J)
38. Hayes JJ, Clark DJ, Wolffe AP (1991) Histone contributions to the structure of DNA in the nucleosome. *Proc Natl Acad Sci USA* 88:6829–6833. doi:[10.1073/pnas.88.15.6829](https://doi.org/10.1073/pnas.88.15.6829)
39. Widom J, Finch JT, Thomas JO (1985) Higher-order structure of long repeat chromatin. *EMBO J* 4:3189–3194
40. Horowitz RA, Agard DA, Sedat JW, Woodcock CL (1994) The three-dimensional architecture of chromatin in situ: electron tomography reveals fibers composed of a continuously variable zig-zag nucleosomal ribbon. *J Cell Biol* 125:1–10. doi:[10.1083/jcb.125.1.1](https://doi.org/10.1083/jcb.125.1.1)
41. Leuba SH, Yang G, Robert C, Samori B, van Holde K, Zlatanova J, Bustamante C (1994) Three-dimensional structure of extended chromatin fibers as revealed by tapping-mode scanning force microscopy. *Proc Natl Acad Sci USA* 91:11621–11625. doi:[10.1073/pnas.91.24.11621](https://doi.org/10.1073/pnas.91.24.11621)
42. Woodcock CL, Dimitrov S (2001) Higher-order structure of chromatin and chromosomes. *Curr Opin Genet Dev* 11:130–135. doi:[10.1016/S0959-437X\(00\)00169-6](https://doi.org/10.1016/S0959-437X(00)00169-6)
43. Schiessel H, Gelbart WM, Bruinsma R (2001) DNA folding: structural and mechanical properties of the two-angle model for chromatin. *Biophys J* 80:1940–1956. doi:[10.1016/S0006-3495\(01\)76164-4](https://doi.org/10.1016/S0006-3495(01)76164-4)
44. Luger K (2003) Structure and dynamic behavior of nucleosomes. *Curr Opin Genet Dev* 13:127–135. doi:[10.1016/S0959-437X\(03\)00026-1](https://doi.org/10.1016/S0959-437X(03)00026-1)
45. Bennink ML, Leuba SH, Leno GH, Zlatanova J, de Grooth BG, Greve J (2001) Unfolding individual nucleosomes by stretching single chromatin fibers with optical tweezers. *Nat Struct Biol* 8:606–610. doi:[10.1038/89646](https://doi.org/10.1038/89646)
46. Brower-Toland B, Wacker DA, Fulbright RM, Lis JT, Kraus WL, Wang MD (2005) Specific contributions of histone tails and their acetylation to the mechanical stability of nucleosomes. *J Mol Biol* 346:135–146. doi:[10.1016/j.jmb.2004.11.056](https://doi.org/10.1016/j.jmb.2004.11.056)
47. Pope LH, Bennink ML, van Leijenhurst-Groener KA, Nikova D, Greve J, Marko JF (2005) Single chromatin fiber stretching reveals physically distinct populations of disassembly events. *Biophys J* 88:3572–3583. doi:[10.1529/biophysj.104.053074](https://doi.org/10.1529/biophysj.104.053074)
48. Cairns BR (2007) Chromatin remodeling: insights and intrigue from single-molecule studies. *Nat Struct Mol Biol* 14:989–996. doi:[10.1038/nsmb1333](https://doi.org/10.1038/nsmb1333)
49. Yan J, Maresca TJ, Skoko D, Adams CD, Xiao B, Christensen MO, Heald R, Marko JF (2007) Micromanipulation studies of chromatin fibers in *Xenopus* egg extracts reveal ATP-dependent chromatin assembly dynamics. *Mol Biol Cell* 18:464–474. doi:[10.1091/mbc.E06-09-0800](https://doi.org/10.1091/mbc.E06-09-0800)
50. Zinchenko AA, Sakaue T, Araki S, Yoshikawa K, Baigl D (2007) Single-chain compaction of long duplex DNA by cationic nanoparticles: modes of interaction and comparison with chromatin. *J Phys Chem B* 111:3019–3031. doi:[10.1021/jp067926z](https://doi.org/10.1021/jp067926z)